Article

Porous ZnO-$ZnAl_2O_4$-CuO Nanocomposites Synthesized by Polymer-Salt Method for Photocatalytic Water Purification and Splitting

Andrey Shelemanov [1*], Artiom Tincu[1], Sergey Evstropiev[1,2,3], Nikolay Nikonorov [1] and Vladimir Vasilyev [1]

[1] ITMO University;
[2] Saint-Petersburg State Technological Institute (Technical University), Saint-Petersburg, Russia
[3] JVC "RPA Vavilov State Optical Institute, Saint-Petersburg, Russia
* Correspondence: shelemanov@mail.ru;

Abstract: In this work, the adsorption and photocatalytic properties of ZnO-$ZnAl_2O_4$-CuO nanosized composites synthesized by the polymer-salt method have been studied. To evaluate the efficiency of adsorption, experiments were carried out on the decolorization of aqueous solutions of the Chicago Sky Blue diazo dye. The adsorption process is divided into two stages, at the first stage the dye is rapidly adsorbed on the outer surface of the composite particles, at the second stage the dye diffuses into the pores of the material. It was noted that the rate of photocatalytic decomposition of the dye is higher than the rate of the adsorption process, which indicates the occurrence of photocatalytic decomposition of dye molecules both on the surface of the composites and in the liquid phase. With an increase in the light intensity, the photocatalytic process is significantly accelerated, linearly at low intensities, and at high intensities the dependence becomes a power law.

Keywords: adsorption; photocatalysis; kinetics; ZnO; nanoparticle

1. Introduction

Photocatalytic processes are widely studied and used for water and air purification, water splitting and other practical applications[1–5]. Nanomaterials based on ZnO are effective photocatalysts which are used for water and air purification [4–11].

It is known that photocatalytic process includes the light absorption by semiconductor, generation of electron-hole pairs, formation of chemically active oxygen species (hydroxyl radicals ·OH, singlet oxygen, etc.) which oxidize organic contaminations on the surface of photocatalyst [1–3,12]. Therefore, the role of different processes proceeding on the semiconductor's surface during photocatalytic processes is very important. The increase of material's specific surface area at the application of nanoscale semiconductors promotes their photocatalytic activity.

The decrease of the size of semiconductors ZnO crystals can be achieved by the optimization of their synthesis conditions [11,13] or by the formation of mixed photocatalytic ZnO-R_xO_y composites (R=Mg,Al,Y,Sn, etc.) [14–16]. The simultaneous formation of different crystals prohibits their growth and the aggregation and provides the formation of the material structure consisting of small particles with high specific surface area.

ZnO-$ZnAl_2O_4$-CuO nanocomposites having high bactericidal properties were synthesized and studied in [17]. $ZnAl_2O_4$ nanoparticles demonstrate high photocatalytic properties [18–26] that determined their application as a component of prepared composite. Cu additions improve photocatalytic properties of $ZnAl_2O_4$ [27].

The study of the features of kinetics of dye adsorption and photooxidation in the solutions containing additions of ZnO-$ZnAl_2O_4$-CuO composites is the aim of this work.

Preprints (www.preprints.org) | NOT PEER-REVIEWED | Posted: 17 February 2023 doi:10.20944/preprints202302.0308.v1

2. Materials and Methods

The polymer-salt method which is applied for the synthesis of different nanoparticle [13,14,28,29] was used in this study. The aqueous solutions of $Zn(NO_3)_2$, $Al(NO_3)_3$ and $CuSO_4$ were used as raw materials for the nanocomposites synthesis. The solution of polyvinylpyrrolidone (PVP) (K30; M_w = 25000÷35000) in propanol-2 was added to the mixture of aqueous solutions of metal salts. Liquid mixtures were stirred for 30 minutes at room temperature. After drying obtained polymer-salt composites were calcined in air atmosphere at 680°C for 2 hours. Chemical compositions of initial solutions and obtained composites are given in Table 1.

Sample	Chemical composition of solutions, wt.%						Chemical composition of powders, mol.%		
	H_2O	PVP	Propanol-2	$Zn(NO_3)_2 \cdot 6H_2O$	$Al(NO_3)_3 \cdot 6H_2O$	$CuSO_4 \cdot 5H_2O$	ZnO	$ZnAl_2O_4$	CuO
1	51.6	2.58	40.6	3.38	1.77	0.013	82.9	16.7	0.4
2	53.0	2.65	41.7	1.76	3.54	0.011	-	99.6	0.4

The morphology of composites was studied by SEM analysis using microscope Supra 55VP. The diffractometer Rigaku Ultima IV was used for X-ray diffraction (XRD) analysis of prepared materials. The crystallite size was calculated using the Scherrer's equation:

$$d = \frac{0.9\,\lambda}{\beta\,\cos\theta}, \quad (1)$$

where d is the average grain size of the crystallites, λ - the incident wavelength, θ - the Bragg angle (radians) and β is the full width at half maximum (FWHM) in radians.

Diazo dye Chicago Sky Blue (CSB) (Sigma Aldrich) was used as model organic contamination in adsorption and photocatalytic experiments. This dye was used earlier for the estimation of photocatalytic properties of different materials [28,29]. The mass of the powder portions used in the experiments was 0.01 g. The powder portions were mixed with 3 ml of an aqueous dye solution (all dye solutions will be aqueous) and placed in a quartz cuvette. Dye content in the initial solutions was 41 mg/l.

3. Results and discussion

3.1. Crystal structure and morphology of ZnO-$ZnAl_2O_4$-CuO composites

Fig.3 shows the SEM images of composites ***1*** (Zn4 Cu0.5) (a,b) and ***2*** (Zn1 Cu0.5) (c,d) at different magnifications. Both composites consist of small nanoparticles that determine the high value of their specific surface area. Composite ***1*** consist of small nanoparticles many of them having shape rods (Fig.1 a,b). A numerous pores are observed in the structure of composite ***2*** (Fig.2c,d). Observed difference in powders morphologies is determined by the chemical compositions of prepared powders.

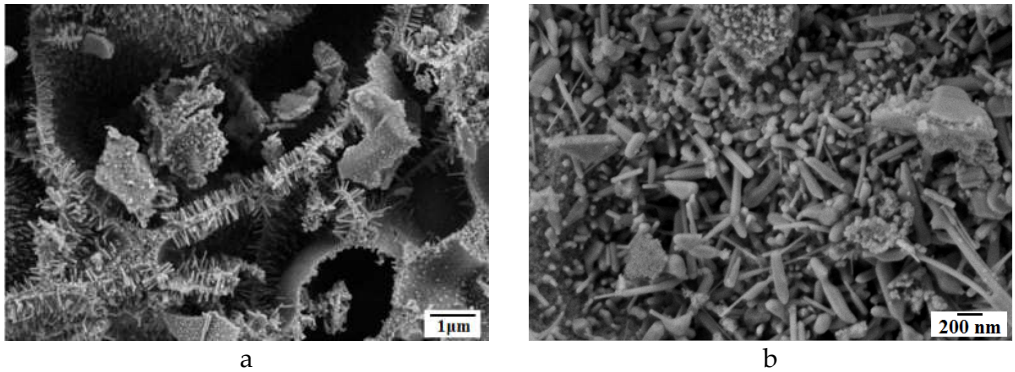

a b

Figure 1. SEM images of composites **1** (a,b) and **2** (c,d) at different magnifications.

Preprints (www.preprints.org) | NOT PEER-REVIEWED | Posted: 17 February 2023 doi:10.20944/preprints202302.0308.v1

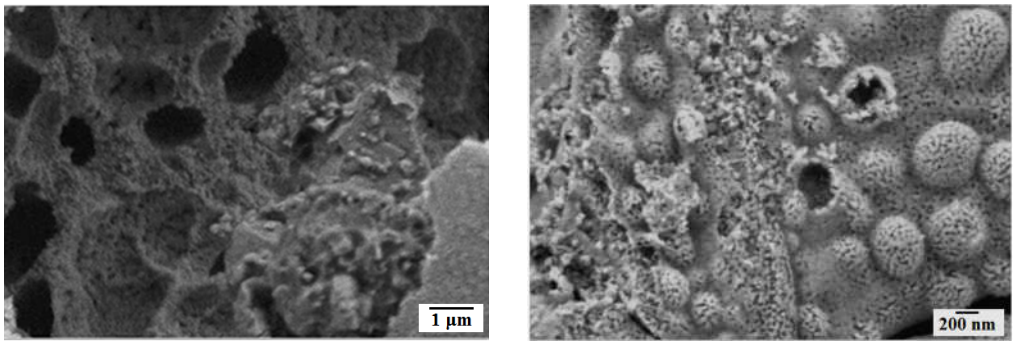

a b

Figure 2. SEM images of composite **2** at different magnifications.

3.2. Photostimulated discoloration of dye solutions

3.2.1. Photolysis of dye molecules in solutions

Figure 3 demonstrates the influence of UV irradiation on the absorption spectra of CSB solutions without addition of composite (a) and with the addition of powder **2** (b). The intensity of dye absorption band (λ_{max} = 612 nm) decreases in spectra of both solutions under UV irradiation.

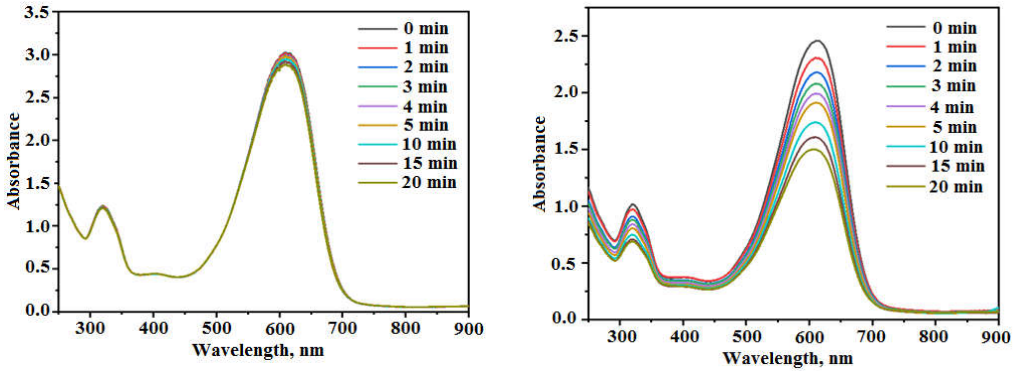

a b

Figure 3. Influence of UV irradiation on the absorption spectra of CSB solutions without addition of composite (a) and with the addition of powder **2** (b).

The changes of absorption spectra of CSB solution without addition of photocatalytic composite are determined by the dye photolysis in the solution. Figure 3a shows that these changes are small after 20 min of UV irradiation. Dye photolysis is photochemical reaction proceeding without photocatalyst. The kinetics of this process is described often by the equation of pseudo-first order:

$$C = C_0 \times e^{-kt}, \quad (1)$$

where C and C_0 – current and initial dye concentrations; k – constant rate of photochemical reaction; t – time.

Figure 3b exposes the effect of UV irradiation on absorption spectra of CSB solution containing powder **2**. It is seen that the shape of dye absorption spectra is remained during irradiation. This fact suggests that forming intermediate products of dye decomposition haven't remarkable light absorption in visible spectral range. The behavior of spectral changes is similar to that reported for CSB photodecomposition in solutions with other photocatalysts [28,29].

3.2.2. Photocatalytic discoloration of dye solutions

Kinetic dependence of the photodecoloration of CSB solution without photocatalytic additions is shown in Figure 4 (curve 1). The decomposition of CSB in solution without

Preprints (www.preprints.org) | NOT PEER-REVIEWED | Posted: 17 February 2023 doi:10.20944/preprints202302.0308.v1

photocatalysts proceeding slowly – less than 4% of dye molecules were decomposed after UV treatment during 20 minutes. Experimental data are described by the equation pseudo-first order (1) with the constant rate k = 0.002 min^{-1} and determination coefficient R^2 = 0.9319. Obtained experimental data showed that photolysis of dye molecules in the solutions without photocatalytic additions is slow process and the input of this process in the total dye decomposition during photocatalytic process is small.

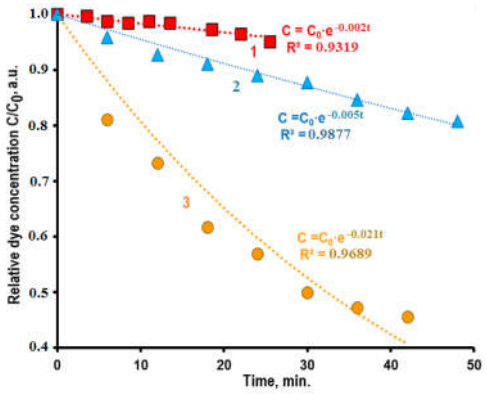

Figure 4. *Kinetics dependencies of CSB solution discoloration during UV irradiation without powders (curve 1) and CSB solutions containing powders* ***2*** *(curve 2) and* ***1*** *(curve 3).*

The rates of photocatalytic dye oxidation (Figure 4, curves 2 and 3) significantly higher than the rate of dye photolysis without photocatalysts (curve 1). The input of the last process in the total dye decomposition during photocatalytic process is small. The significant difference of dye decomposition rates observed at the use of composites 1 and 2 related to difference of their chemical composition and morphology (fig.1 and 2).

The Langmuir-Hinshelwood (L-H) kinetic model is used often to describe semiconductor photocatalysis [1,30]. According to this model the dye decomposition rate r is described by kinetic equation: [1–4,28–31]:

$$r = -\frac{dC}{dt} = \frac{k_1 K_a C}{1+K_a C}, \quad (2)$$

where C – current dye concentration at the time t, k_1 – constant rate of dye decomposition, K_a – constant of adsorption-desorption equilibrium. At low dye content (C << 1 mM), the equation (1) is simplified to pseudo-first order equation [32,33]:

$$ln(C|C_0) = k_1 K_a t = k_{app} t, \quad (3)$$

where k_{app} – apparent constant rate of pseudo-first order. Kinetics dependencies of the photodecomposition of CSB in the solutions containing additions of powders of are described sufficiently by the equation (3) with determination coefficients R^2 = 0.9689 and 0.9877 for composites ***1*** and ***2***, correspondingly. These results are agreed with the data of the work [34] in which was demonstrated that L-H model correspond to the kinetics of photodecomposition of an azo dye by porous photocatalysts at the initial stages of the process.

3.2.3. Dye adsorption from solutions on the surfaces of composites

Observed solutions discoloration at the presence of photocatalytic composites is determined by a few different processes:

1. The dye photolysis in the liquid phase;
2. Its adsorption on the powder surface;
3. Photocatalytic dye decomposition.

Preprints (www.preprints.org) | NOT PEER-REVIEWED | Posted: 17 February 2023 doi:10.20944/preprints202302.0308.v1

Figure 5a demonstrates changes of absorption spectra of dye solution containing powder ***1*** during adsorption process in the darkness. The behavior of these changes is similar to that observed during UV irradiation of dye solutions. Approximately 25-30% of dye molecules are adsorbed on the surface of the composite ***1*** during first 120 min of adsorption process. It is worth to notice that adsorption process and solution discoloration are continued for 1 week (Fig.5a).

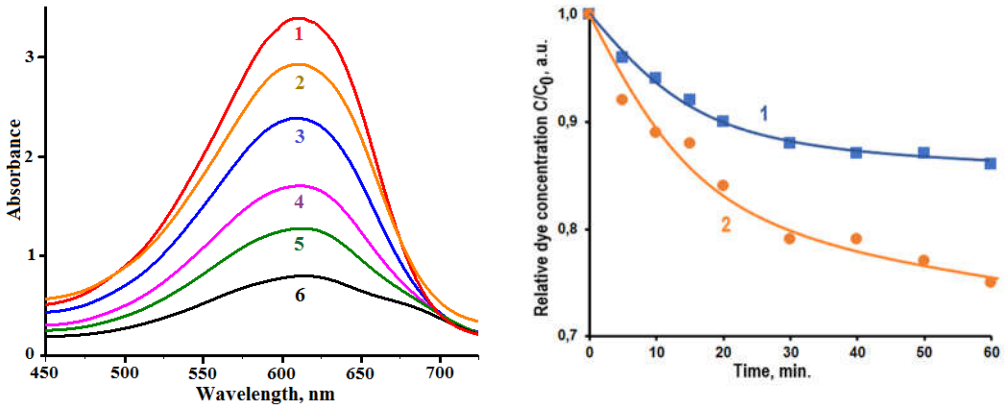

a b

Figure 5. a Changes of absorption spectra of dye solution containing powder 1 (Zn4-1) during adsorption process. Adsorption duration, min: 0 (curve 1); 20 (curve 2); 120 (curve 3); 1440 (curve 4); 2880 (curve 5); 10080 (curve 6), **b** Kinetic dependencies of the dye adsorption on the powders **2** (curve 1) and **1** (curve 2).

Kinetic models of adsorption on the surface of photocatalysts are used at the consideration of photocatalytic processes. The relatively simple kinetic models including the equations of the pseudo-first or pseudo-second orders are used often [28,35].

The adsorption rate can be described the kinetic equation of pseudo-first order [28,36,37]:

$$\frac{dq_t}{dt} = k_f \times (q_e - q_t), \quad (4)$$

where q_t – the dye amount adsorbed by 1 g of the sorbent at the time t; q_e – equilibrium adsorption capacity; k_f – rate constant of the adsorption; t – adsorption duration. According to equation (4) the rate of the adsorption decreases as the surface is filled with dye molecules.

It is necessary to pay attention to the value of the equilibrium adsorption capacity q_e, which enters into the equation (4). In some works [37,38] the q_e is assigned a value determined as a result of short-term experiments (1÷2 hours) by approximating the kinetic dependence based on the observed decrease in the adsorption rate. The data shown in Fig.5a indicate that the achievement of adsorption-desorption equilibrium on the surface of ZnO-$ZnAl_2O_4$-CuO composites requires a much longer adsorption process.

Fig.6 demonstrates the dependence $\ln(q_e - q_t) = f(t)$ for the dye adsorption on the surface of composite ***1*** during 48 hours. This long-term dependence is described formally by kinetic equation (4) with $k_1 = 0.0007$ min^{-1} and $R^2 = 0.9525$. However, the experimental points obtained at initial stages of the adsorption deviate significantly from the linear dependence that indicates that adsorption process has the complicate behavior.

Preprints (www.preprints.org) | NOT PEER-REVIEWED | Posted: 17 February 2023 doi:10.20944/preprints202302.0308.v1

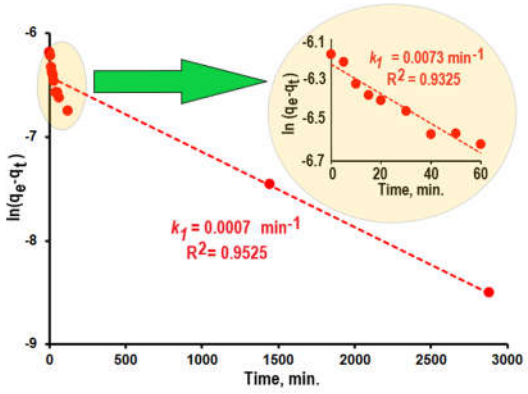

Figure 6. Dependence $\mathbf{ln(q_e - q_t) = f(t)}$ for the dye adsorption on the surface of composite **1**. **Inset**: Dependence $\mathbf{ln(q_e - q_t) = f(t)}$ for initial stages of the dye adsorption on the surface of composite **1**.

The inset in Fig.6 shows the dependence $\boldsymbol{ln(q_e - q_t) = f(t)}$ for initial stages of the dye adsorption on the surface of composite ***1***. The rate of adsorption in these stages is significantly (more than 10 times) higher ($\boldsymbol{k_f}$= 0.0073 min^{-1}) than average value.

Based on obtained data the kinetics of adsorption process can be separated to two different stages:

1. Fast adsorption observed at initial stages of the process (duration of adsorption ~ 120 min.);
2. Slow adsorption which is proceed at more long-term process (duration of adsorption > 120 min.).

It is possible to suggests that dye molecules fust adsorb on the external surface of composite particles at the first stage of the process. Following slow adsorption is determined by the labored diffusion of dye molecules into the tiny pores and caverns inside composites particles.

For the description of adsorption kinetics, the equation of pseudo-second order is often used also. This equation can be written as:

$$\frac{dq_t}{dt} = k_2 \times (q_e - q_t)^2, \quad (5)$$

and in the integral form [31,32,39]:

$$\frac{t}{q_t} = \frac{1}{k_2 \times q_e^2} + \frac{t}{q_e}, \quad (6)$$

where $\boldsymbol{k_2}$ - rate constant of the adsorption, $\boldsymbol{q_e}$ – equilibrium adsorption capacity, $\boldsymbol{q_t}$ – the dye amount adsorbed by 1 g of the sorbent at the time ***t***. This model describes a much stronger dependence of the adsorption rate on coverage degree of sorbent surface with dye molecules. The graphs $\boldsymbol{t/q = f(t)}$ for the kinetics of dye adsorption on the surface of composite ***1*** showed a satisfactory agreement ($\boldsymbol{R^2}$ = 0.9899) between experimental data and equation (6) (Fig.7).

Preprints (www.preprints.org) | NOT PEER-REVIEWED | Posted: 17 February 2023 doi:10.20944/preprints202302.0308.v1

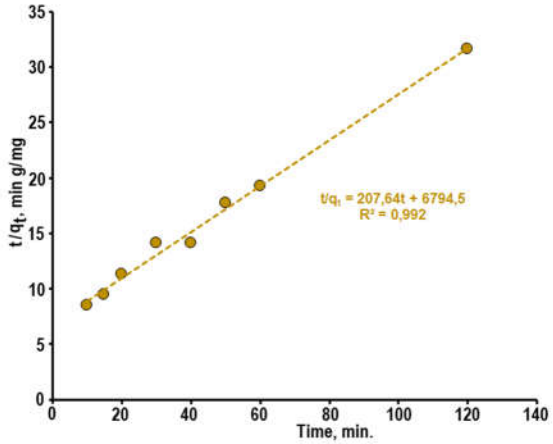

Figure 7. Dependence **$t/q_t = f(t)$**, based on the experimental data of dye adsorption on the surface of the composite **1**.

Based on the obtained results it is possible to conclude that the adsorption of diazo dye CSB from the aqueous solutions on the surface of porous ZnO-$ZnAl_2O_4$-CuO composites can be described by both kinetic models pseudo-first and pseudo-second orders.

3.2.4. The ratio of adsorption and photocatalysis rates

Usually, the reactant species adsorption is considered as the first stage of photocatalytic process in a typical photocatalytic reaction [40,41]. Dye adsorption and its photodecomposition are considerate as successive stages of photocatalysis. Therefore, the total rate of photocatalytic dye decomposition couldn't be higher the adsorption rate. However, this is not agreed with obtained experimental results.

Fig.8 shows kinetic dependencies of dye adsorption from the solution on the surface of composites ***1*** (curve 1) and ***2*** (curve 2) and the dye photocatalytic decomposition using composites ***1*** (curve 3) and ***2*** (curve 4). It is worth to notice that experimental data showed in Fig.8 indicate thar photocatalytical dye decomposition proceeds faster than dye adsorption process. This phenomenon was observed earlier in [28] and was explained by the oxidation of some part of dye molecules in liquid phase by the chemically active oxygen species photogenerated by photocatalyst. Photocatalytic degradation of the organic contaminant in aqueous solution using composite photocatalyst was observed also in [42]. Thus, it is possible to conclude that at the application of porous ZnO-$ZnAl_2O_4$-CuO composites photocatalytic dye degradation proceeds as on the surface of photocatalysts so as in the liquid phase.

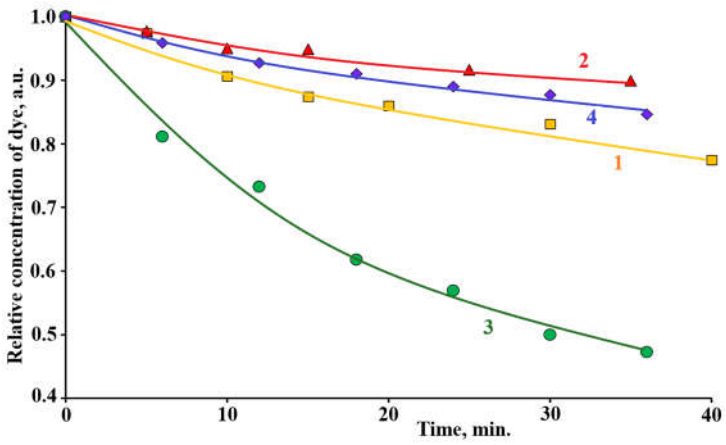

Figure 8. Kinetic dependencies of dye adsorption from the solution on the surface of composites **1** (curve 1) and **2** (curve 2) and the dye photocatalytic decomposition using composites **1** (curve 3) and **2** (curve 4).

Preprints (www.preprints.org) | NOT PEER-REVIEWED | Posted: 17 February 2023 doi:10.20944/preprints202302.0308.v1

3.2.5. Influence of the light intensity on the kinetics of photocatalysis

It is known that the light is the driving force of photocatalytic processes. Influence of light intensity ***I*** on the kinetics of photocatalytic decomposition of different organic compounds was studied in many works [1–9]. It was found that at the application of L-H model obtained values k_1 and K_a are dependent from the light intensity ***I*** and different approaches were used to describe these dependences. Deng [1] and Puma et al. [9] separates the dependence $r = f(I)$ to a few different regions determining by ***I*** values. At low light intensity a linear dependence of photodecomposition rate ***r*** from the light intensity ***I*** is observed ($r \propto I$) [1]. At the increase of light intensity linear dependence $r = f(I)$ transforms to a power law dependence $r \propto I^{\beta}$ $(0 \le \beta < 1)$ [1].

These features of $r = f(I)$ dependencies are determined by the mechanisms of the processes proceeding at the semiconductor photocatalyst excitation. Photogenerated electron-hole pairs can recombine directly, or they can be trapped by the matter and take part in photocatalytic process. Clearly, that high light intensity and more trapping of electron-hole pairs may increase the dye decomposition rate. The trapping of the electron-hole pairs and photocatalytic action dominate at low light intensity values while the recombination processes prevail at high light intensity values [1,10].

The dependence of $k_{app} = f(I)$ for photocatalytic dye degradation using composite ***1*** is exposes in Fig.9. At the low light intensity, the dependence is linear but at I > 100 mW/cm^2 it transforms to a power law dependence. Observed behavior of $k_{app} = f(I)$ dependence fully corresponds to the literature data.

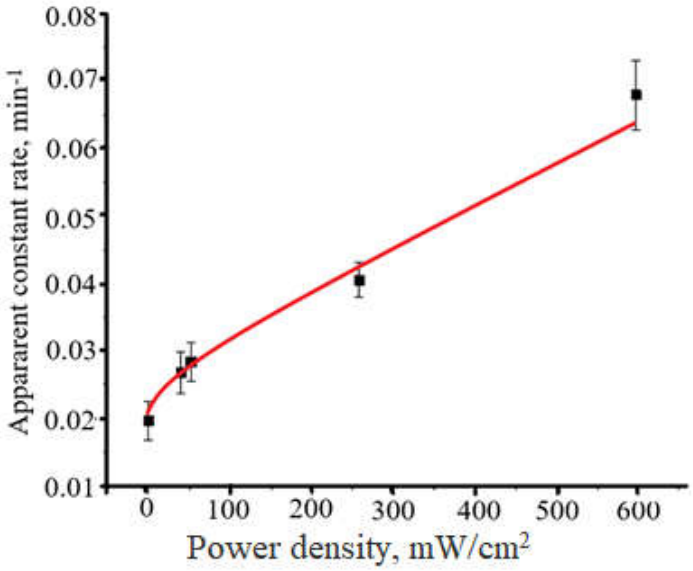

Figure 9. The dependence of $k_{app} = f(I)$ for photocatalytic dye degradation using composite

4. Conclusions

ZnO-ZnAl2O4 composites synthesized by polymer-salt method consists of small (size less 100 nm) nanoparticles, have "pine needles"-like or porous structure and demonstrate some features of their adsorption and photocatalytic properties. Experiments on the adsorption diazo dye Chicago Sky Blue from aqueous solutions on the surface of prepares composites showed that adsorption kinetics consists of two different stages. The first stage of this process is the fast dye adsorption on the external surface of composites particles followed by the slow diffusion and dye adsorption inside pores and caverns. The rate of photocatalytic dye decomposition is higher than the rate of adsorption process. It suggests the photocatalytic decomposition of dye molecules proceeds as on the surface of composites so as in the liquid phase.

 doi:10.20944/preprints202302.0308.v1

The increase of light intensity significantly accelerates the photocatalytic process. At the low light intensity, the dependence is linear but at I > 100 mW/cm^2 it transforms to a power law dependence.

Author Contributions:

Conceptualization, Andrey Shelemanov and Sergey Evstropiev;

methodology, Artyom Tincu and Andrey Shelemanov.;

validation, Nikolay Nikonorov.;

formal analysis, Sergey Evstropiev;

investigation, Artyom Tincu and Andrey Shelemanov;

resources, Sergey Evstropiev and Nikolay Nikonorov;

data curation, Andrey Shelemanov and Sergey Evstropiev;

writing—original draft preparation, Sergey Evstropiev.

writing—review and editing, Andrey Shelemanov;

visualization, Andrey Shelemanov and Sergey Evstropiev;

supervision, Nikolay Nikonorov and Vladimir Vasilyev

project administration, Andrey Shelemanov.;

funding acquisition, Sergey Evstropiev and Nikolay Nikonorov.

All authors have read and agreed to the published version of the manuscript.

Funding: This research was funded by the Russian Science Foundation grant number 20-19-00559.

Conflicts of Interest: The authors declare no conflict of interest. The funders had no role in the design of the study; in the collection, analyses, or interpretation of data; in the writing of the manuscript; or in the decision to publish the results.

References

1. Deng, Y. Developing a Langmuir-Type Excitation Equilibrium Equation to Describe the Effect of Light Intensity on the Kinetics of the Photocatalytic Oxidation. *Chem. Eng. J.* **2018**, *337*, 220–227, DOI:10.1016/j.cej.2017.12.059.
2. Mills, A.; Wang, J.; Ollis, D. Dependence of the Kinetics of Liquid-Phase Photocatalyzed Reactions on Oxygen Concentration and Light Intensity. *J. Catal.* **2006**, *243*, 1–6, DOI:10.1016/j.jcat.2006.06.025.
3. Yang, L.; Liu, Z. Study on Light Intensity in the Process of Photocatalytic Degradation of Indoor Gaseous Formaldehyde for Saving Energy. *Energy Convers. Manag.* **2007**, *48*, 882–889, DOI:10.1016/j.enconman.2006.08.023.
4. Bell, S.; Will, G.; Bell, J. Light Intensity Effects on Photocatalytic Water Splitting with a Titania Catalyst. *Int. J. Hydrog. Energy* **2013**, *38*, 6938–6947, DOI:10.1016/j.ijhydene.2013.02.147.
5. Jadaa, W.; Prakash, A.; Ray, A.K. Photocatalytic Degradation of Diazo Dye over Suspended and Immobilized TiO2 Catalyst in Swirl Flow Reactor: Kinetic Modeling. *Processes* **2021**, *9*, 1741, DOI:10.3390/pr9101741.
6. Meng, Y.; Huang, X.; Wu, Y.; Wang, X.; Qian, Y. Kinetic Study and Modeling on Photocatalytic Degradation of Para-Chlorobenzoate at Different Light Intensities. *Environ. Pollut.* **2002**, *117*, 307–313, DOI:10.1016/S0269-7491(01)00184-1.
7. Xu, Y.; Langford, C.H. Variation of Langmuir Adsorption Constant Determined for TiO2-Photocatalyzed Degradation of Acetophenone under Different Light Intensity. *J. Photochem. Photobiol. Chem.* **2000**, *133*, 67–71, DOI:10.1016/S1010-6030(00)00220-3.
8. Li, Y.; Sun, S.; Ma, M.; Ouyang, Y.; Yan, W. Kinetic Study and Model of the Photocatalytic Degradation of Rhodamine B (RhB) by a TiO2-Coated Activated Carbon Catalyst: Effects of Initial RhB Content, Light Intensity and TiO2 Content in the Catalyst. *Chem. Eng. J.* **2008**, *142*, 147–155, DOI:10.1016/j.cej.2008.01.009.
9. Li Puma, G.; Salvadó-Estivill, I.; Obee, T.N.; Hay, S.O. Kinetics Rate Model of the Photocatalytic Oxidation of Trichloroethylene in Air over TiO2 Thin Films. *Sep. Purif. Technol.* **2009**, *67*, 226–232, DOI:10.1016/j.seppur.2009.03.011.
10. Turchi, C. Photocatalytic Degradation of Organic Water Contaminants: Mechanisms Involving Hydroxyl Radical Attack. *J. Catal.* **1990**, *122*, 178–192, DOI:10.1016/0021-9517(90)90269-P.
11. Wang, X.; Ahmad, M.; Sun, H. Three-Dimensional ZnO Hierarchical Nanostructures: Solution Phase Synthesis and Applications. *Materials* **2017**, *10*, 1304, DOI:10.3390/ma10111304.
12. Li, Y.; Zhang, W.; Niu, J.; Chen, Y. Mechanism of Photogenerated Reactive Oxygen Species and Correlation with the Antibacterial Properties of Engineered Metal-Oxide Nanoparticles. *ACS Nano* **2012**, *6*, 5164–5173, DOI:10.1021/nn300934k.
13. Shelemanov, A.A.; Evstropiev, S.K.; Karavaeva, A.V.; Nikonorov, N.V.; Vasilyev, V.N.; Podruhin, Y.F.; Kiselev, V.M. Enhanced Singlet Oxygen Photogeneration by Bactericidal ZnO–MgO–Ag Nanocomposites. *Mater. Chem. Phys.* **2022**, *276*, 125204, DOI:10.1016/j.matchemphys.2021.125204.
14. Evstropiev, S.K.; Karavaeva, A.V.; Petrova, M.A.; Nikonorov, N.V.; Vasilyev, V.N.; Lesnykh, L.L.; Dukelskii, K.V. Antibacterial Effect of Nanostructured ZnO-SnO2 Coatings: The Role of Microstructure. *Mater. Today Commun.* **2019**, *21*, 100628, DOI:10.1016/j.mtcomm.2019.100628.
15. Hamrouni, A.; Moussa, N.; Parrino, F.; Di Paola, A.; Houas, A.; Palmisano, L. Sol–Gel Synthesis and Photocatalytic Activity of ZnO–SnO2 Nanocomposites. *J. Mol. Catal. Chem.* **2014**, *390*, 133–141, DOI:10.1016/j.molcata.2014.03.018.
16. Manoharan, C.; Pavithra, G.; Dhanapandian, S.; Dhamodharan, P. Effect of In Doping on the Properties and Antibacterial Activity of ZnO Films Prepared by Spray Pyrolysis. *Spectrochim. Acta. A. Mol. Biomol. Spectrosc.* **2015**, *149*, 793–799, DOI:10.1016/j.saa.2015.05.019.
17. Tincu, A.; Shelemanov, A.A.; Evstropiev, S.K.; Nikonorov, N.V.; Dukelskii, K.V. Controlled Chemical Transformation and Crystallization Design for the Formation of Multifunctional Cu-Doped ZnO/ZnAl2O4 Composites. *J. Inorg. Organomet. Polym. Mater.* **2022**, DOI:10.1007/s10904-022-02507-6.
18. Foletto, E.L.; Battiston, S.; Simões, J.M.; Bassaco, M.M.; Pereira, L.S.F.; de Moraes Flores, É.M.; Müller, E.I. Synthesis of ZnAl2O4 Nanoparticles by Different Routes and the Effect of Its Pore Size on the Photocatalytic Process. *Microporous Mesoporous Mater.* **2012**, *163*, 29–33, DOI:10.1016/j.micromeso.2012.06.039.

19. Anchieta, C.G.; Sallet, D.; Foletto, E.L.; da Silva, S.S.; Chiavone-Filho, O.; do Nascimento, C.A.O. Synthesis of Ternary Zinc Spinel Oxides and Their Application in the Photodegradation of Organic Pollutant. *Ceram. Int.* **2014**, *40*, 4173–4178, DOI:10.1016/j.ceramint.2013.08.074.
20. Battiston, S.; Rigo, C.; Severo, E. da C.; Mazutti, M.A.; Kuhn, R.C.; Gündel, A.; Foletto, E.L. Synthesis of Zinc Aluminate (ZnAl2O4) Spinel and Its Application as Photocatalyst. *Mater. Res.* **2014**, *17*, 734–738, DOI:10.1590/S1516-14392014005000073.
21. Zawadzki, M.; Staszak, W.; López-Suárez, F.E.; Illán-Gómez, M.J.; Bueno-López, A. Preparation, Characterisation and Catalytic Performance for Soot Oxidation of Copper-Containing ZnAl2O4 Spinels. *Appl. Catal. Gen.* **2009**, *371*, 92–98, DOI:10.1016/j.apcata.2009.09.035.
22. Zhao, X.; Wang, L.; Xu, X.; Lei, X.; Xu, S.; Zhang, F. Fabrication and Photocatalytic Properties of Novel ZnO/ZnAl2O4 Nanocomposite with ZnAl2O4 Dispersed inside ZnO Network. *AIChE J.* **2012**, *58*, 573–582, DOI:10.1002/aic.12597.
23. Shahmirzaee, M.; Shafiee Afarani, M.; Arabi, A.M.; Iran Nejhad, A. In Situ Crystallization of ZnAl2O4/ZnO Nanocomposite on Alumina Granule for Photocatalytic Purification of Wastewater. *Res. Chem. Intermed.* **2017**, *43*, 321–340, DOI:10.1007/s11164-016-2624-6.
24. Yuan, X.; Cheng, X.; Jing, Q.; Niu, J.; Peng, D.; Feng, Z.; Wu, X. ZnO/ZnAl2O4 Nanocomposite with 3D Sphere-Like Hierarchical Structure for Photocatalytic Reduction of Aqueous Cr(VI). *Materials* **2018**, *11*, 1624, DOI:10.3390/ma11091624.
25. Zhang, L.; Yan, J.; Zhou, M.; Yang, Y.; Liu, Y.-N. Fabrication and Photocatalytic Properties of Spheres-in-Spheres ZnO/ZnAl2O4 Composite Hollow Microspheres. *Appl. Surf. Sci.* **2013**, *268*, 237–245, DOI:10.1016/j.apsusc.2012.12.069.
26. Zhao, H.; Dong, Y.; Jiang, P.; Wang, G.; Zhang, J.; Zhang, C. ZnAl2O4 as a Novel High-Surface-Area Ozonation Catalyst: One-Step Green Synthesis, Catalytic Performance and Mechanism. *Chem. Eng. J.* **2015**, *260*, 623–630, DOI:10.1016/j.cej.2014.09.034.
27. Akika, F.Z.; Benamira, M.; Lahmar, H.; Trari, M.; Avramova, I.; Suzer, Ş. Structural and Optical Properties of Cu-Doped ZnAl2O4 and Its Application as Photocatalyst for Cr(VI) Reduction under Sunlight. *Surf. Interfaces* **2020**, *18*, 100406, DOI:10.1016/j.surfin.2019.100406.
28. Saratovskii, A.S.; Bulyga, D.V.; Evstrop'ev, S.K.; Antropova, T.V. Adsorption and Photocatalytic Activity of the Porous Glass–ZnO–Ag Composite and ZnO–Ag Nanopowder. *Glass Phys. Chem.* **2022**, *48*, 10–17, DOI:10.1134/S1087659622010126.
29. Evstropiev, S.K.; Lesnykh, L.V.; Karavaeva, A.V.; Nikonorov, N.V.; Oreshkina, K.V.; Mironov, L.Yu.; Maslennikov, S.Yu.; Kolobkova, E.V.; Vasilyev, V.N.; Bagrov, I.V. Intensification of Photodecomposition of Organics Contaminations by Nanostructured ZnO-SnO2 Coatings Prepared by Polymer-Salt Method. *Chem. Eng. Process. - Process Intensif.* **2019**, *142*, 107587, DOI:10.1016/j.cep.2019.107587.
30. Fox, M.Anne.; Dulay, M.T. Heterogeneous Photocatalysis. *Chem. Rev.* **1993**, *93*, 341–357, DOI:10.1021/cr00017a016.
31. Gaya, U.I.; Abdullah, A.H. Heterogeneous Photocatalytic Degradation of Organic Contaminants over Titanium Dioxide: A Review of Fundamentals, Progress and Problems. *J. Photochem. Photobiol. C Photochem. Rev.* **2008**, *9*, 1–12, DOI:10.1016/j.jphotochemrev.2007.12.003.
32. Konstantinou, I.K.; Albanis, T.A. TiO2-Assisted Photocatalytic Degradation of Azo Dyes in Aqueous Solution: Kinetic and Mechanistic Investigations. *Appl. Catal. B Environ.* **2004**, *49*, 1–14, DOI:10.1016/j.apcatb.2003.11.010.
33. Vimonses, V.; Chong, M.N.; Jin, B. Evaluation of the Physical Properties and Photodegradation Ability of Titania Nanocrystalline Impregnated onto Modified Kaolin. *Microporous Mesoporous Mater.* **2010**, *132*, 201–209, DOI:10.1016/j.micromeso.2010.02.021.
34. Ibhadon, A.O.; Greenway, G.M.; Yue, Y.; Falaras, P.; Tsoukleris, D. The Photocatalytic Activity and Kinetics of the Degradation of an Anionic Azo-Dye in a UV Irradiated Porous Titania Foam. *Appl. Catal. B Environ.* **2008**, *84*, 351–355, DOI:10.1016/j.apcatb.2008.04.019.
35. Jose, L.M.; Raj, R.S.A.; Sajan, D.; Aravind, A. Adsorption and Photocatalytic Activity of Biosynthesised ZnO Nanoparticles Using Aloe Vera Leaf Extract. *Nano Express* **2021**, *2*, 010039, DOI:10.1088/2632-959X/abeec6.
36. Lagergren, S. *About the Theory of So-Called Adsorption of Soluble Substances*; Kung Sven Veten Hand.; Vol. 24:1;

37. Kuang, Y.; Zhang, X.; Zhou, S. Adsorption of Methylene Blue in Water onto Activated Carbon by Surfactant Modification. *Water* **2020**, *12*, 587, DOI:10.3390/w12020587.
38. Minh, T.T.; Tu, N.T.T.; Van Thi, T.T.; Hoa, L.T.; Long, H.T.; Phong, N.H.; Pham, T.L.M.; Khieu, D.Q. Synthesis of Porous Octahedral ZnO/CuO Composites from Zn/Cu-Based MOF-199 and Their Applications in Visible-Light-Driven Photocatalytic Degradation of Dyes. *J. Nanomater.* **2019**, *2019*, 1–16, DOI:10.1155/2019/5198045.
39. Uribe-López, M.C.; Hidalgo-López, M.C.; López-González, R.; Frías-Márquez, D.M.; Núñez-Nogueira, G.; Hernández-Castillo, D.; Alvarez-Lemus, M.A. Photocatalytic Activity of ZnO Nanoparticles and the Role of the Synthesis Method on Their Physical and Chemical Properties. *J. Photochem. Photobiol. Chem.* **2021**, *404*, 112866, DOI:10.1016/j.jphotochem.2020.112866.
40. *Surface Science of Photocatalysis*; Yu, J., Jaroniec, M., Jiang, C., Eds.; Interface science and technology; Academic Press, an imprint of Elsevier: London, United Kingdom ; San Diego, CA, United States, 2020; ISBN 978-0-08-102890-2.
41. Abebe, B.; Murthy, H.C.A.; Amare, E. Summary on Adsorption and Photocatalysis for Pollutant Remediation: Mini Review. *J. Encapsulation Adsorpt. Sci.* **2018**, *08*, 225–255, DOI:10.4236/jeas.2018.84012.
42. El Mouchtari, E.M.; Bahsis, L.; El Mersly, L.; Anane, H.; Lebarillier, S.; Piram, A.; Briche, S.; Wong-Wah-Chung, P.; Rafqah, S. Insights in the Aqueous and Adsorbed Photocatalytic Degradation of Carbamazepine by a Biosourced Composite: Kinetics, Mechanisms and DFT Calculations. *Int. J. Environ. Res.* **2021**, *15*, 135–147, DOI:10.1007/s41742-020-00300-2.